

A study on micro machining of e-glass–fibre–epoxy composite by ECSM process

Alakesh Manna · Vivek Narang

Received: 6 June 2011 / Accepted: 4 January 2012 / Published online: 12 April 2012
© Springer-Verlag London Limited 2012

Abstract The paper presents the result of an experimental investigation on the micro machining of electrically non-conductive e-glass–fibre–epoxy composite during electrochemical spark machining using specially designed square cross section with centrally micro hole brass tool and different diameter round-shaped micro tools made of IS-3748 steel. A micro electrochemical spark machining (ECSM) setup has been designed, fabricated and used for conducting the experiments. According to the Taguchi method-based design, the specific numbers of experiments have been carried out to investigate the influence of the fabricated ECSM parameters on the material removal rate and overcut on generated hole radius. Test results show that the material removal rate is maximum when machining was performed at higher setting value of D.C. supply voltage (e.g. 70 V), moderate setting value of electrolytic concentration (e.g. 80 g/l) and 180-mm gap between electrodes. Taking significant machining parameters into consideration and using multiple linear regression, mathematical models for material removal rate and overcut on hole radius are established to investigate the influence of cutting parameters during micro-ECSM. The influence of machining parameters on machined hole and special shape contour quality are also analysed through different scanning electron micrographs. Confirmation test results established the fact that the developed mathematical models are appropriate for effectively representing the machining performance criteria.

Keywords E-glass–fibre–epoxy composite · ECSM · MRR · SEM photo

1 Introduction

Advance engineering materials are gradually becoming very important for their scope and use in advance manufacturing industries due to their high fatigue strength, thermal shock resistance, high strength-to-weight ratio, etc. However, high values of these properties make it more difficult to form into a desired shape by well-known conventional machining methods, thereby limiting their widespread applications. Ceramics and fibre-reinforced polymer composites have very attractive properties. But e-glass–fibre–epoxy composite is an electrically non-conductive material and conventional machining of fibre–epoxy composites leads to delamination and fuzzing. Even non-conventional machining processes like electric discharge machining (EDM), electrochemical machining (ECM), WEDM, etc. are not suitable to machine such material because of its non-conductivity of electricity property. To overcome this constraint, a hybrid process has been conceived, in which the phenomenon of electrochemical spark is employed for material removal from electrically non-conducting materials. A combined technique of electrochemical (ECM) and EDM known as electrochemical spark machining (ECSM) has been designed, fabricated and thereafter utilised to machine the electrically non-conductive e-glass–fibre–epoxy composite.

The basic principle of material removal in ECSM process is electrochemical dissolution of the workpiece in the presence of electrical spark discharge action created by applying sufficient D.C. voltage to the electrolytic cell in proper polarity, i.e. positive terminal connected to the anode (i.e. auxiliary electrode) and negative terminal connected to the

A. Manna (✉) · V. Narang
Department of Mechanical Engineering,
Punjab Engineering College (Deemed University),
Chandigarh 160012, India
e-mail: kgpmanna@rediffmail.com

Table 1 Summary of experimental conditions

Machine tool used	Developed micro electrochemical spark machining (ECSM) setup
Electrolyte used	Sodium hydroxide (NaOH)
Concentration	(1) 65 g of NaOH/litre of dematerialized deionised water (2) 70 g of NaOH/litre of dematerialized deionised water (3) 75 g of NaOH/litre of dematerialized deionised water (4) 80 g of NaOH/litre of dematerialized deionised water
Workpiece	Electrically non-conductive e-glass–fibre–epoxy composite (size, 40×16×2.5 mm)
Cathode (tool)	IS-3748/T35Cr5Mo1V30 with diameter of 400 μm

cathode. When the applied voltage reaches beyond a certain level, reduction of electrolyte takes place and liberates hydrogen gas bubbles at the cathode and generates electrolytic gas around the surface of the electrode. There is evolution of oxygen gas and formation of oxide films at the auxiliary electrode surface while machining of electrically non-conducting materials.

From the literature survey, it is evident that some of researches on electrochemical machining have been carried out by the previous researchers but still a lot of applied research in the above field is required so as to explore the successful utilisations of the process in the area of machining of non-electrically conductive materials. Keeping in view of some of the published research, works in brief are listed below.

The spark energy and the approximate order of hydrogen gas bubble diameter are computed utilising proposed valve theory via analysis of ECSM process by Jain et al. [1]. During trepanning of Al_2O_3 , by electrochemical discharge machining, Chak et al. [2] observed that machining performance gradually deteriorates with an increase in tool depth and finally caused micro cracks on the machined surface due to thermal shocks at high voltage. During ECSM of glass workpiece, Bhondwe et al. [3] observed that the material removal rate (MRR) is increased with an increase in soda lime electrolyte concentration. Basak and Ghosh [4] developed a theoretical model of the discharge phenomenon and estimated the critical voltage and current required to initiate discharge between the electrode and the electrolyte for spark generation during electrochemical discharge machining. Jain et al. [5] studied on the electrochemically spark abrasive

drilling and reported that electrochemical spark machining with abrasive cutting tools gives better performance for machining of electrically non-conducting materials, alumina and borosilicate glass. Bhattacharyya et al. [6] stated that an appreciable amount of MRR and lesser overcut can be possible to generate during electrochemical machining when parametric setting values varies between 10 and 15 ms pulse on time and 15–20 g/l electrolyte concentration. ECDM yields higher machining rate over ECM or EDM claimed by Mediliyegedara et al. [7]. Schöpf et al. [8] stated that the ECDM process can be used for truing and dressing of metal-bonded diamond grinding tools. Han et al. [9] explained the improvement of surface integrity of electrochemical discharge machining process using powder-mixed electrolyte. They stated that fine graphite powder mixed with electrolyte gives better surface integrity. The pulsed D.C. power proved better spark stability and more spark energy release than constant D.C. power during slicing of optical glass claimed by Peng and Liao [10]. The electrochemical micro machining can be effectively used for high-precision machining operations, i.e. for accuracies of the order of $\pm 1 \mu\text{m}$ on $50 \mu\text{m}$ claimed by Bhattacharyya et al. [11].

Table 2 Developed ECDM parameters and their levels for machining of micro holes

Parameters, their symbols and units	Parametric levels			
	1	2	3	4
A: D.C. supply voltage (X_1 , V)	55	60	65	70
B: Electrolyte concentration (X_2 , g/l)	65	70	75	80
C: Gap between tool and anode (X_3 , mm)	200	190	180	170

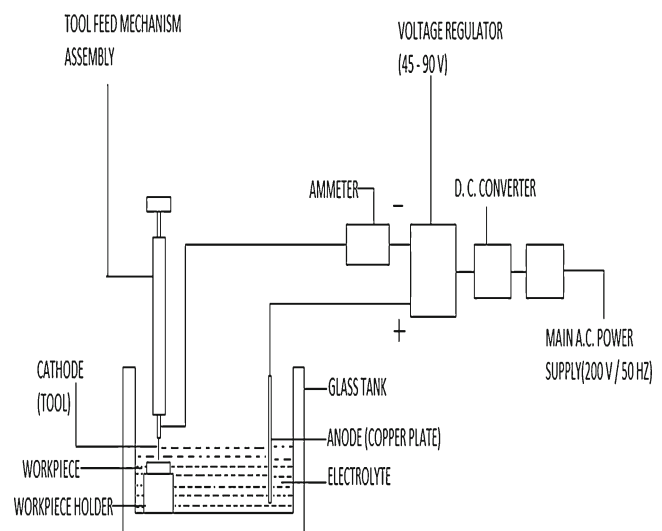
**Fig. 1** Schematic diagram of the ECSM system

Table 3 L₁₆ (4⁵) orthogonal array, coded values of different parameters and results

Exp. no.	Parametric levels and their coded values			Experimental results and S/N ratio for MRR (mg/min) and overcut on hole radius (Woc; mm)						
	X ₁ : Col-1	X ₂ : Col-2	X ₃ : Col-3	MRR (Y ₁)	MRR (Y ₂)	MRR (Y ₃)	Average MRR (Y)	S/N ratio for MRR, η (dB)	Average Woc (mm)	S/N ratio for Woc, η (dB)
1	1	1	1	1.37	1.316	1.262	1.0195	-1.0823	0.0355	27.7006
2	1	2	2	1.906	1.798	1.852	1.32225	1.1649	0.0402	26.6214
3	1	3	3	2.49	2.544	2.436	1.83925	4.0360	0.0495	24.8351
4	1	4	4	1.232	1.178	1.124	2.49525	6.6896	0.0642	22.5782
5	2	1	2	1.482	1.374	1.428	1.18675	0.2218	0.0452	25.6114
6	2	2	1	2.116	2.17	2.062	1.42125	1.7939	0.0545	24.0034
7	2	3	4	2.77	2.716	2.662	2.117	5.2608	0.069	21.9595
8	2	4	3	1.49	1.382	1.436	2.681	7.3071	0.0885	19.8011
9	3	1	3	1.766	1.82	1.712	1.428	1.8348	0.0497	24.7925
10	3	2	4	2.44	2.386	2.332	1.7575	3.6416	0.0655	22.4124
11	3	3	1	2.844	2.736	2.79	2.3675	6.2307	0.0755	21.1816
12	3	4	2	1.69	1.744	1.636	2.77825	7.6229	0.0942	19.2581
13	4	1	4	2.444	2.39	2.336	1.67025	3.1941	0.0605	23.0998
14	4	2	3	2.668	2.56	2.614	2.36525	6.2205	0.0797	20.7073
15	4	3	2	3.002	3.056	2.948	2.6135	7.0923	0.1032	18.4620
16	4	4	1	1.37	1.316	1.262	2.97525	8.2158	0.1200	17.1632

2 Experimental planning

An electrochemical spark machining setup has been designed and fabricated for conducting the experiments. Micro holes of different diameters were performed on electrically non-conductive e-glass–fibre–epoxy composite using developed ECSM setup.

Table 1 presents the summary of the developed machining setup, workpiece and electrolyte used for experimentation. Table 2 shows the different parameters and their levels considered for experimental investigation. The Taguchi method-based robust design L₁₆ (4⁵) orthogonal array was used for experimental investigation [12]. The material removal rates were determined by difference of weight of workpieces before and after each hole. Sartorius Master

Series Electronic Balance of least count of 0.01 mg was used to weight the workpieces before and after each run. The depths of holes were measured by utilising a Mitutoyo digital vernier calliper with a resolution of 0.01 mm. Different scanning electron micrographs (SEMs) of the micro-machined holes were taken to analyse the surface texture of the machined hole. Each test sample was cut into two pieces along the centre line of the each hole with necessary precaution so that inner surface does not get damaged.

3 Design and development of micro ECDM setup

A schematic diagram of the developed ECSM system is shown in Fig. 1. Other equipment are utilised (not shown

Table 4 ANOVA for MRR and Woc

Sr/No.	Control factor	Analysis for material removal rate (MRR)					Overcut on hole radius (Woc; mm)				
		SS	DOF	V	F ₀	Percentage of cont.	SS	DOF	V	F ₀	Percentage of cont.
1	A	4.8527	3	1.61757	155.81	20.57	0.01556	3	0.00519	159.61	44.43
2	B	18.0126	3	6.00421	578.36	76.38	0.01724	3	0.00575	176.84	49.22
3	C	0.1562	3	0.05208	5.02	0.68	0.00047	3	0.00016	4.86	1.36
4	Error	0.5606	54	0.01038		2.37	0.00175	54	0.00003		4.99
5	Total	23.5822	63			100	0.03502	63			100

A DC supply voltage (X₁), B electrolyte concentration (X₂), C Gap between tool and anode (X₃)

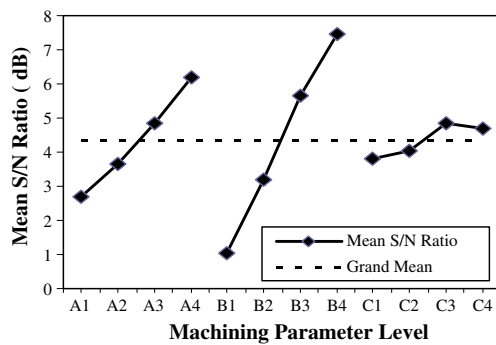


Fig. 2 *S/N* ratio graph for MRR, in milligrams per minute

here) such as: (a) tank for electrolyte concentration, (b) workpiece holder, (c) D.C. generator with regulator to supply the constant D.C. voltage at various levels and (d) step-down transformer for supply of 18 V to run the stepper motor mounted on fabricated micro-ECSM setup.

A D.C. generator is used to convert 220 V A.C. into D.C. supply in the range of 45 to 90 V. The main supply A.C.—220 V—is stepped down to 18 V by utilising a step-down transformer for operating a stepper motor. The 18-V stepper motor is utilised to give the feed motion of the electrode. An automatic feed motion control circuit is designed, manufactured and used for the purpose. A scale is fixed along the side of the electrolyte chamber to measure the gap between micro tool, i.e. electrode and copper anode. An insulated tool holder was adopted to hold the electrode and installed inside the electrolyte tank.

4 Results and discussions

The test results are analysed to identify the most effective parameters of the developed ECSM setup. Different SEMs show the characteristics of the machined micro holes

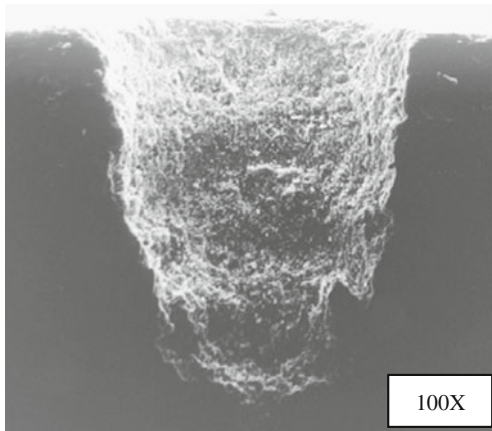


Fig. 3 SEM of an orthogonal cutting section

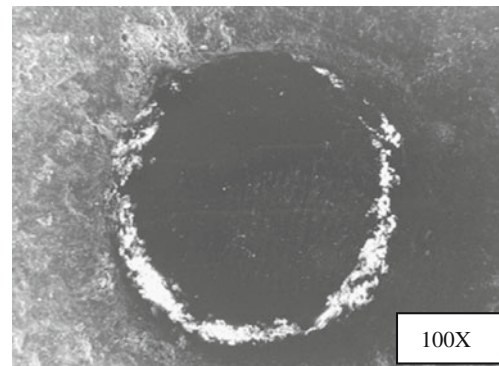


Fig. 4 SEM graph of a through micro hole

generated during ECSM operation. According to the Taguchi method, $L_{16} (4^5)$ orthogonal array is used for experimental investigation. Table 3 presents the $L_{16} (4^5)$ orthogonal array, coded values of the different parameters, experimental results and *S/N* ratios for MRR (in milligrams per minute) and overcut on hole radius (*Woc*; in millimetres).

Table 4 shows the ANOVA and “*F* test” values with percentage of contribution, i.e. effectiveness of the individual machining parameter on MRR and overcut on hole radius, i.e. micro hole gap width over hole radius (*Woc*; in millimetres). From Table 4, it is clear that the electrolyte concentration has the most significant effect on MRR with an *F* test value of 578.36 and 76.38 % contribution. The parameter D.C. supply voltage has 20.57 % contribution with 155.81 *F* test value on MRR. From Table 4, it is also clear that the electrolyte concentration and D.C. supply voltage are the most significant and significant parameters with *F* test values of 176.84 (contribution 49.22 %) and 159.61, (contribution 44.43 %) respectively, on overcut on hole radius.

Utilising the different values of *S/N* ratios (η , in decibel) for material removal rate (Table 3), *S/N* ratio curves were drawn as shown in Fig. 2. From Fig. 2, it is concluded that optimal parametric combination for maximum MRR is

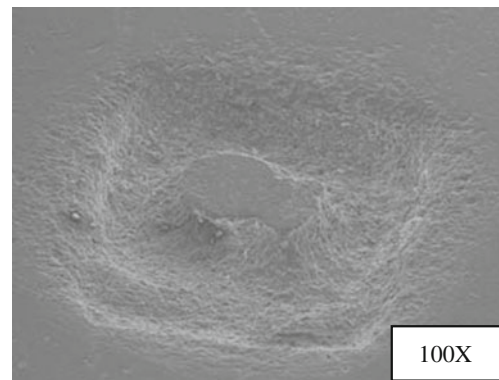


Fig. 5 SEM of a generated special contour shape on e-glass-fibre-epoxy composite

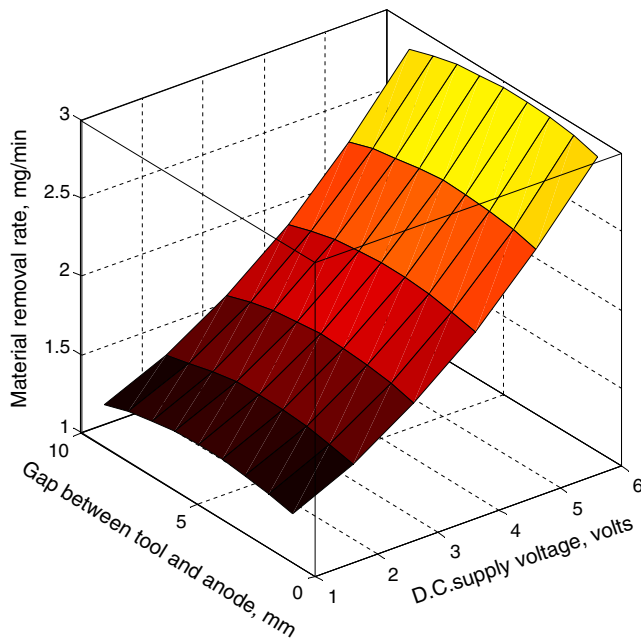


Fig. 6 Interaction effect of gap between electrodes and supply voltage on MRR

$A_4B_4C_3$. Similarly, the *S/N* ratio curve for micro hole overcut on hole radius was drawn (not shown in the paper) and it was found that the optimal parametric combination for minimum overcut on hole radius (*Woc*; in millimetres) is $A_4B_4C_4$.

Figure 3 shows an SEM of an orthogonal cutting section of a micro-machined hole generated during drilling of e-glass–fibre–epoxy composite on designed and developed ECSM setup. The orthogonal cutting section was taken for SEM on generated micro hole with parametric setting at 55 V D.C. supply voltage, 65 g/l electrolyte concentration and 200-mm gap between anode and cathode. The orthogonal cutting section shown in Fig. 3 was a result of continuous 5 min of machining with 400- μ m-diameter micro tool. From the SEM in Fig. 3, it is clear that the shape of the generated micro hole is conical in nature and surface generated is poor.

Figure 4 shows an SEM of a through machined hole generated during machining of e-glass–fibre–epoxy composite on designed and fabricated ECSM setup. This through hole was generated with parametric setting at 70 V D.C.

supply voltage, 80 g/l electrolyte concentration and 170-mm gap between anode and cathode. The hole shown in Fig. 4 was a result of continuous 20 min of machining with 400- μ m-diameter tool. From Fig. 4, it is concluded that the generated hole is oval in shape and deposition of e-glass fibre like white foam is observed on the outer periphery of the generated hole. It may be due to the accumulation of heated and deformed uncut and un-burnt epoxy fibres around the tool during machining but not cleaned out properly by the flashing of electrolyte.

A brass tool with a central micro hole (not shown here) was used for machining of special contour micro hole with centrally projected parent metal on e-glass–fibre–epoxy composite. The brass tool used for this purpose has a 850 \times 850- μ m square cross section with a central 400- μ m-diameter micro hole of 1-mm depth. Figure 5 shows an SEM of a generated contour shape on e-glass–fibre–epoxy composite during machining by designed and fabricated ECSM setup. The contour shape was generated with parametric setting at 60 V D.C. supply voltage, 100 g/l electrolyte concentration and 200-mm gap between anode and cathode. The contour shape shown in Fig. 5 was a result of continuous 15 min of machining with centrally micro hole brass tool.

From the experimental results and SEM, it is clear that micro drilling proceeds in an asymmetrical shape. Burrs are noticed on the surface of the hole, which proves that machining of very fine micro hole on e-glass–fibre–epoxy composite is possible but may compromise with the excellent accuracy. The particles of the material are observed scattered along the depth due to electrical sparking. At the beginning, the micro hole was exactly round in shape and its diameter is about equal to the electrode diameter, but after that, it is reduced along the depth of the hole. Debris and white foam are also noticed along the whole depth of the generated hole.

5 Development of mathematical models

Considering the significant machining parameters, mathematical models for MRR and overcut on hole radius are developed. The additivity test results show that the predicted

Table 5 Additivity test condition, results and percentage of error

Exp. no.	ECSM parameters			MRR, mg/min			Spark gap width (<i>Woc</i>), mm		
	X_1	X_2	X_3	Experimental	Developed Eq. 1	Percentage of error	Experimental	Developed Eq. 2	Percentage of Error
1	57	68	195	1.369	1.2764	6.764	0.061	0.0579	5.0819
2	62	73	185	2.048	1.9856	3.0468	0.082	0.0783	4.5121
3	67	78	175	3.056	2.8895	5.4482	0.123	0.1153	6.2601

determined values utilising developed mathematical models make a good agreement with the experimental results.

Mathematical model for MRR (in milligrams per minute) is

$$Y_{\text{MRR}} = -31.225374 - 0.050318 \cdot X_1 + 0.286611 \cdot X_2 + 0.205940 \cdot X_3 - 0.000832 \cdot X_1 X_2 - 0.000011 \cdot X_1 X_3 - 0.001599 \cdot X_2 X_3 + 0.001408 \cdot X_1^2 + 0.001076 \cdot X_2^2 - 0.000244 \cdot X_3^2$$

$$R^2 = 0.976 \quad (1)$$

where X_1 , X_2 and X_3 are the supply D.C. voltage (in volts), electrolyte concentration (in grams per litre) and gap between tool and anode (in millimetres), respectively.

In Fig. 6, along X -axis, “1” to “6” represent variation in voltage from 50 to 75 V with an increment of 5 Vs, and along Y -axis, “0” to “10” represent variation in gap between anode and tool from 170 to 200 mm with an increment of 15 mm. From Fig. 6, it is clear that the MRR increases slightly with a decrease in gap between electrodes. It is also clear that the MRR increases with an increase in the D.C. supply voltage. From Fig. 6, it is clear that at higher setting, the MRR value of D.C. supply voltage, e.g. 70 V and at moderate setting values of gap between electrodes, e.g. 180 mm, is maximum. The MRR is minimum when the gap between electrodes is maximum, i.e. 200 mm, and supply D.C. voltage is minimum, i.e. 55 V.

Mathematical model for overcut on hole radius (W_{oc} ; in millimetres) is

$$Y_{\text{Woc}} = 0.047491 - 0.012497 \cdot X_1 - 0.006096 \cdot X_2 + 0.004737 \cdot X_3 + 0.000169 \cdot X_1 X_2 + 0.00000018 \cdot X_1 X_3 - 0.000049 \cdot X_2 X_3 + 0.000026 \cdot X_1^2 + 0.000051 X_2^2 - 0.000003 \cdot X_3^2$$

$$R^2 = 0.95 \quad (2)$$

6 Additivity test

Table 5 presents the parametric condition utilised for additivity test to validate the developed mathematical models for MRR and W_{oc} (in millimetres) during machining of e-glass–fibre–epoxy composite using developed ECSM setup. This table also represents the percent of error of the calculated values utilising developed models with respect to the experimental results.

7 Conclusions

Based on the experimentally obtained results during machining of electrically non-conductive e-glass–fibre–epoxy composites on designed and fabricated ECDM setup and

thereafter discussion on the investigated results, the following conclusions are drawn as listed below.

1. The electrolyte concentration has the most significant effect on material removal rate and overcut on hole radius with an F test value of 578.36, contribution of 76.38 % and F test value of 176.84 and contribution of 49.22 %, respectively. The D.C. supply voltage has a significant effect on MRR and overcut on hole radius with an F test value of 155.81, contribution of 20.57 % and an F test value of 159.61 and contribution of 44.43 %, respectively.
2. For maximum material removal rate, the optimal parametric combination is $A_4 B_4 C_3$, i.e. MRR is maximum at the parametric combination of 70 V D.C. supply voltage, 80 g/l electrolytic concentration and 180-mm gap between anode and cathode.
3. The surface generated during micro drilling of e-glass–fibre–epoxy composite is very poor. The reinforced epoxy fibres are not completely cut during machining, rather they are burnt and integrated. Many of them cause rough fabric surface which appear in the form of debris. It is also observed during machining that the generated hole is oval in shape. The shape of the generated micro hole along its depth is conical in nature and the surface generated is poor.
4. The generation of a special contour shape on e-glass–fibre–epoxy composites is possible by electrochemical discharge machining process.

References

1. Jain VK, Dixit PM, Pandey PM (1999) On the analysis of the electrochemical spark machining process. *Int J Mach Tool Manufact* 39:165–186
2. Chak SK, Rao PV (2007) Trepanning of Al_2O_3 by electrochemical discharge machining (ECDM) process using abrasive electrode with pulsed DC supply. *Int J Mach Tool Manufact* 47:2061–2070
3. Bhondwe KL, Yadava V, Kathiresan G (2006) Finite element prediction of material removal rate due to electro-chemical spark machining. *Int J Mach Tool Manufact* 46(14):1699–1706
4. Basak I, Ghosh A (1997) Mechanism of material removal in electrochemical discharge machining: a theoretical model and experimental verification. *J Mater Process Tech* 71(3):350–359
5. Jain VK, Choudhury SK, Ramesh KM (2002) On the machining of alumina and glass. *Int J Mach Tool Manufact* 42:1269–1276
6. Bhattacharyya B, Munda J (2003) Experimental investigation on the influence of electrochemical machining parameters on machining rate and accuracy in micromachining domain. *Int J Mach Tool Manufact* 43:1301–1310
7. Mediliyegedara TKKR, De SAKM, Harrison DK, McGeough JA (2005) New developments in the process control of the hybrid electro chemical discharge machining (ECDM) process. *J Mater Process Tech* 167(2–3):338–343

8. Schöpf M, Beltrami I, Boccadoro M, Kramer D, Schumacher B (2001) ECDM (electro chemical discharge machining), a new method for trueing and dressing of metal bonded diamond grinding tools. *CIRP Ann Manuf Technol* 50(1):125–128
9. Han M-S, Min B-K, Lee Sang Jo (2007) Improvement of surface integrity of electro-chemical discharge machining process using powder-mixed electrolyte. *J Mater Process Tech* 191(1–3):224–227
10. Peng WY, Liao YS (2004) Study of electrochemical discharge machining technology for slicing non-conductive brittle materials. *J Mater Process Tech* 149:363–369
11. Bhattacharyya B, Munda J, Malapati M (2004) Advancement in electrochemical micro-machining. *Int J Mach Tool Manufact* 44:1577–1589
12. Montgomery DC (1997) *Design and analysis of experiments*. Wiley, New York